Immunity to infection

Basic

Research Article

TLR9 signalling inhibits *Plasmodium* liver infection by macrophage activation

Maximilian Kordes[1] (ID)*, Louise Ormond[2], Sebastian Rausch[3],
Kai Matuschewski[1,4]* (ID) *and Julius Clemence R. Hafalla[2]* (ID)

[1] Parasitology Unit, Max Planck Institute for Infection Biology, Berlin, Germany
[2] Department of Infection Biology, Faculty of Infectious and Tropical Diseases, London School of Hygiene and Tropical Medicine, London, United Kingdom
[3] Institute of Immunology, Centre of Infection Medicine, Freie Universität Berlin, Berlin, Germany
[4] Department of Molecular Parasitology, Institute of Biology, Humboldt University, Berlin, Germany

Recognition of pathogen-associated molecular patterns (PAMPs) through Toll-like receptors (TLRs) plays a pivotal role in first-line pathogen defense. TLRs are also likely triggered during a *Plasmodium* infection in vivo by parasite-derived components. However, the contribution of innate responses to liver infection and to the subsequent clinical outcome of a blood infection is not well understood. To assess the potential effects of enhanced TLR-signalling on *Plasmodium* infection, we systematically examined the effect of agonist-primed immune responses to sporozoite inoculation in the *P. berghei*/C57Bl/6 murine malaria model. We could identify distinct stage-specific effects on the course of infection after stimulation with two out of four TLR-ligands tested. Priming with a TLR9 agonist induced killing of pre-erythrocytic stages in the liver that depended on macrophages and the expression of inducible nitric oxide synthase (iNOS). These factors have previously not been recognized as antigen-independent effector mechanisms against *Plasmodium* liver stages. Priming with TLR4 and -9 agonists also translated into blood stage-specific protection against experimental cerebral malaria (ECM). These insights are relevant to the activation of TLR signalling pathways by adjuvant systems of antimalaria vaccine strategies. The protective role of TLR4-activation against ECM might also explain some unexpected clinical effects observed with pre-erythrocytic vaccine approaches.

Keywords: innate immunity · *Plasmodium* infection · malaria · TLR9 signaling · macrophages

Additional supporting information may be found online in the Supporting Information section at the end of the article.

Introduction

Malaria, caused by the apicomplexan parasite *Plasmodium*, continues to be one of the most urgent public health problems worldwide [1]. Severe forms of malaria, including cerebral malaria (CM), mostly affect children and naïve individuals, who have not yet acquired partial antiparasite immunity or disease tolerance. In these individuals, nonadaptive immune mechanisms are crucial to control the infection, but the host's immune response is also involved in severe immunopathology [2–4].

Correspondence: Dr. Julius Clemence R. Hafalla
e-mail: Julius.Hafalla@lshtm.ac.uk

During natural malaria transmission, infective sporozoites are inoculated during blood feeding by an infected female *Anopheles* mosquito. Sporozoites migrate in the skin, enter a capillary blood vessel, infect hepatocytes, and undergo asexual replication in the liver to form merozoites, which are released into the blood stream. These merozoites infect erythrocytes for further rounds of schizogony and ultimately form sexual stages that can be retransmitted to the mosquito vector. While blood stages are associated with high numbers of parasites, clinical signs and complications, pre-erythrocytic stages form a bottleneck in the *Plasmodium* life cycle, and are considered clinically and immunologically silent [5, 6].

Malaria-related morbidity and mortality are mainly attributed to complications of infections with *P. falciparum*, which can cause severe anemia, respiratory distress, severe hypoglycemia, CM, or combinations thereof [7]. CM is marked by a deterioration of the patient's neurological status leading to coma. CM is a result of the sequestration of infected red blood cells (iRBC) to the brain microvasculature, a dysregulation of proinflammatory cytokines, brain swelling, and vascular dysfunction [8]. As a surrogate experimental model of CM, murine *Plasmodium* infections resulting in experimental CM (ECM) are widely used [9]. In this model, C57Bl/6 mice are infected with *P. berghei* (*Pb*; strain ANKA) and develop ataxia, paralysis, seizures, and coma 6–11 days after infection. This disease model has revealed important pathomechanisms, such as dysregulation of the proinflammatory cytokines gamma IFN (IFN-γ) [10], tumor necrosis factor (TNF) [11], and lymphotoxin [12] and migration of CD-8$^+$ T cells to the microvasculature of the brain [13, 14].

Toll-like receptors (TLRs) are a conserved group of pattern recognition receptors (PRRs) that play pivotal roles in the recognition of pathogen-derived components and initiation of innate immune signalling pathways [15]. Different TLRs have distinct molecular ligand specificities to pathogen-associated molecular patterns (PAMPs) that are conserved across species [16]. TLR2 is activated by components of the bacterial cell wall, such as lipoteichoic acid and peptidoglycan [17]; TLR3 binds double-stranded (dsRNA) and can be activated by the synthetic analogue polyinosine-polycytidylic acid (poly I:C) [18]; lipopolysaccharide (LPS) of Gram-negative bacteria is sensed by TLR4 [19]; and TLR9 senses unmethylated CpG motifs in bacterial DNA [20].

As ECM has been linked to dysregulation of proinflammatory signals, various studies have attempted to unravel the role of TLRs and their major downstream signalling molecule myeloid differentiation primary response protein 88 (MyD88) in the development of ECM. For malaria infections initiated with iRBCs, mice deficient in MyD88 or TLR1, -2, -3, -4, -6, -7, or -9 [21] or those triple deficient in TLR2, -4 and -9 [22] were found to be as susceptible to ECM as wild-type (WT) mice. In sharp contrast, we, using sporozoite-induced infections, and others, using iRBC-induced infections, observed either partial or almost full protection from ECM in *Pb* ANKA-infected mice deficient in MyD88 or partial protection from ECM in mice deficient in TLR2, combined TLR2/4, TLR7, TLR9 or combined TLR7/9 [23–25]. The latter findings are further supported by in vitro studies in *P. falciparum*, which iden-

tified glycosylphosphatidylinositol (GPI) and hemozoin as candidate ligands for TLR2 and -9, respectively [26, 27], but the correct identification of hemozoin as the malarial TLR9 ligand is controversial [28]. Moreover, the pharmacological inhibition of TLR9 has been suggested as a therapeutic approach to target CM, preventing ECM and increasing survival in the rodent model [29].

The opposite approach —therapies based on TLR agonists— provides a common strategy to target other human diseases including infectious, malignant, autoimmune, and allergic diseases [30]. However, little is known about the effect of enhanced activation of TLRs on the course of malaria infection. Moreover, in a natural transmission setting, the clinical course of a malaria infection remains largely unpredictable. Whether costimulation of the innate immune pathways, *for example*, in coinfections with other pathogens, modulates *Plasmodium* infections and disease dynamics remains unsolved. A single study with *P. yoelii* demonstrated that agonists of TLR2, -3, -4, and -9, respectively, have a partial inhibitory capacity on liver stage growth in BALB/c mice [31]. In this study, oligonucleotides with CpG-motifs, which activate TLR9, also conferred sterile protection against a low-dose inoculum of sporozoites, and the authors attributed the protection to proinflammatory cytokines and Kupffer cell activity [31]. This study also confirmed earlier findings that CpG-oligodeoxynucleotide (ODNs) confers interleukin (IL)-12 and IFN-γ dependent sterile protection against low-dose infection with *P. yoelii* sporozoites [32]. Similarly, the control of murine infections with *Toxoplasma gondii*, an apicomplexan parasite distantly related to *Plasmodium*, depends on early induction of IL-12 from dendritic cells (DCs) and IFN-γ produced by natural killer (NK) cells, which, in this case, is triggered by mouse-specific TLR11 activation [33, 34].

Antigen-specific immunity to pre-erythrocytic stages is well characterized and depends on CD8$^+$ memory T cells and IFN-γ expressed by CD4$^+$ T cells to stimulate the production of inducible nitric oxide synthase 2 (iNOS) and NO in hepatocytes to restrict liver-stage development [33]. Effector mechanisms of antigen-independent responses are, in contrast, less well understood. Hepatic macrophages upregulated IL-12, in response to, a challenge with infectious sporozoites after previous immunization with attenuated sporozoites [34], possibly in response to, priming with PAMPs. In the absence of previous activation, the role of macrophages in liver-stage infection is, however, ambivalent. Sporozoite traverse macrophages to facilitate hepatocyte infection and do not get efficiently cleared in this process [35]. Congruently, viable sporozoites decrease macrophages' antigen presenting cell (APC) function and IL-12 expression [34].

We hypothesized that modulation of *Plasmodium* infections, achieved by activation of TLR pathways prior to infection, is characteristic of distinct pathways. Intriguingly, using the *Pb*/C57Bl/6 infection model, we found that specific TLRs and associated signalling pathways modulate disease progression and severity by distinguishable mechanisms. Our results have wide-ranging implications on our fundamental understanding of inflections in the immune system and their effect on malaria infection, as well as to adjuvant choices for malaria vaccine approaches.

Results

Application of TLR agonists primes the immunological environment to subsequent *Pb* infection

We hypothesized that early innate immune mechanisms are capable of modulating *Plasmodium* infections. We tested this hypothesis in the *Pb* rodent malaria model. Known ligands of TLR2 (peptidoglycan) [17], TLR3 (Poly I:C) [18], TLR4 (LPS) [19], and TLR9 (ODN 1826, an oligonucleotide containing unmethylated CpG motifs) [20] were injected into C57Bl/6 mice to trigger an innate immune response prior to inoculation of *Pb* sporozoites. Additionally, we included a control oligonucleotide with the same sequence as ODN 1826 but with inverted GpC motifs (ODN1826 Control) not recognized by TLR9 to control for potential effects not triggered via this pathway. We also included a group that only received PBS.

To distinguish immunomodulatory effects caused by these reagents from the response caused by infection with *Pb*, we first characterized the immune response elicited 20 h after injection of respective TLR agonists into naïve mice by phenotypic analysis of spleen and liver-derived APCs and lymphocytes (Fig. 1A). Injection of ODN 1826 upregulated CD86 and CD80 expression on splenic CD11c$^+$ (dendritic) cells, and upregulated major histocompatibility complex (MHC) Class II expression on both splenic and liver CD11c$^+$; CD80 expression was downregulated on liver CD11c$^+$ cells (Fig. 1B). Injection of LPS upregulated CD86 and CD80 expression on splenic CD11c$^+$ cells, and upregulated MHC Class II expression on liver CD11c$^+$; MHC II expression was downregulated on splenic CD11c$^+$ cells, as well as CD80 expression on liver CD11c$^+$ cells. Injection of Poly I:C upregulated CD86, CD80, and MHC Class II expression on splenic CD11c$^+$ cells and MHC Class II expression on liver CD11c$^+$ cells, CD80 expression on liver CD11c$^+$ cells was downregulated. Peptidoglycan only upregulated CD80 expression on splenic CD11c$^+$ cells. Injection of ODN 1826, LPS, and Poly I:C upregulated CD86 expression on splenic F4/80$^+$ cells (macrophages); injection of Poly I:C upregulated CD80 expression on these cells. Injection of ODN 1826 upregulated CD86 and MHC Class II expression on liver F4/80$^+$ cells; LPS upregulated CD86$^+$ expression on these cells. Injection of peptidoglycan and ODN 1826 Control barely impacted the upregulation of activation markers for CD11c$^+$ and F4/80$^+$ cells. Based on the upregulation of CD69, ODN 1826, LPS, and poly I:C are potent activators of splenic and liver CD4$^+$ T cells, CD8$^+$ T cells, NK (CD3$^-$ CD49b$^+$) cells, and NK T (CD3$^+$ CD49b$^+$) cells.

Next, we assessed the serum levels of the proinflammatory cytokines IFN-γ, TNF, IL-6, and IL-12p70, as well as the anti-inflammatory IL-10 and the chemokine monocyte chemoattractant protein (MCP)-1, 20 h after injection of respective TLR agonists into naïve mice (Fig. 1C). ODN 1826 application led to significantly elevated levels of IFN-γ ($p = 0.032$), IL-6 ($p = 0.021$), IL-12 ($p = 0.008$), MCP-1 ($p = 0.008$) TNF ($p = 0.012$), and IL-10 ($p = 0.008$). LPS administration significantly induced IL-6 ($p = 0.021$). Injection of poly I:C, peptidoglycan and ODN 1826 Control barely altered any of the measured cytokine levels.

Together, application of TLR agonists, particularly ODN 1826, leads to distinct modulations of the immunological environment, as exemplified by changes in the phenotypes of splenic and liver leucocytes and serum cytokine levels that will be encountered by an incoming pathogen.

Activation of TLR9 pathway modulates *Pb* liver-stage development

After characterization of the immunological responses to prestimulation, we compared the capacity of distinct TLRs to elicit an innate immune response against pre-erythrocytic stages of *Plasmodium*. We focused on the TLR3-, TLR4-, or TLR9-agonists given the poor responses elicited by peptidoglycan in our initial experiments (Fig. 1). We treated mice with poly I:C, LPS, and ODN 1826, and 20 h later, infected them with 10^4 *Pb* sporozoites (Fig. 2A); parasite loads in the liver were assessed by the quantification of the relative amount of parasite 18S ribosomal ribonucleic acid (rRNA) 42 h after infection. Control groups included those that received PBS and OD1826 Control. Stimulation with ODN 1826 reduced the hepatic parasite load by 89% of the average amount found in the PBS-treated control group ($p = 0.0007$) (Fig. 2B). Stimulation with Poly I:C, LPS, and ODN 1826 Control had no effect on hepatic parasite burden ($p > 0.05$).

We also initially confirmed whether the reduction caused by ODN 1826 indeed depends on the innate signalling pathway described for TLR9 [36, 37], by pretreating and infecting WT C57Bl/6 mice and mice deficient for the MyD88 in side-by-side comparison (Supporting information Fig. S1). Consistent with our earlier results, stimulation with the ODN 1826 led to a reduction by 88% in WT controls ($p = 0.0005$), while we did not observe any difference between unstimulated and stimulated MyD88$^{-/-}$ mice ($p = 0.5$). Moreover, there was no difference in the parasite 18S rRNA levels between untreated WT mice and MyD88$^{-/-}$ mice that had received ODN 1826 or PBS (both $p > 0.05$).

Activation of TLR9 pathway does not affect gliding motility of *Plasmodium* sporozoites

To further substantiate our hypothesis that activation of the innate immune system was responsible for the reduction of the hepatic parasite load in vivo, we tested in vitro if direct stimulation of hepatocytes can autonomously limit parasite development. We prestimulated primary mouse hepatocytes for 24h with Poly I:C, LPS, and ODN 1826 and infected them with *Pb* sporozoites. Compared to pretreatment with sterile culture medium or ODN 1826 Control, we did not observe any morphological or quantitative difference in the formation of exoerythrocytic forms (EEF; Fig. 3A and B).

Reports that CpG oligonucleotides are able to inhibit *Plasmodium* gliding motility in vitro [38] also prompted us to consider that this is a possible explanation for the delayed development of pre-erythrocytic stages. Therefore, we tested if LPS and ODN 1826 (versus ODN 1826 Control)—two agonists that either affected
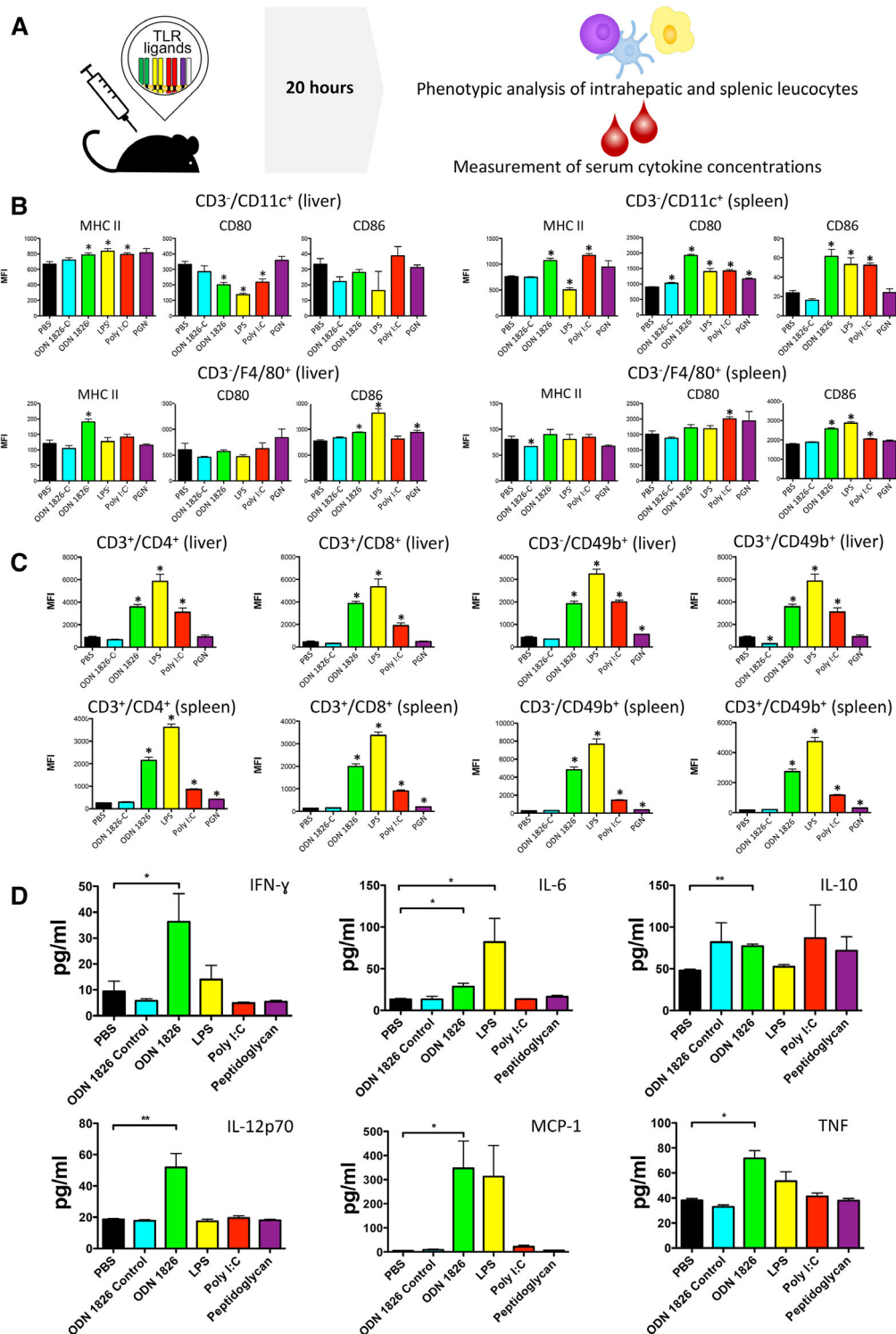
Figure 1. Differential effects of activation of innate immune pathways in naïve mice. **(A)** Flowchart of experimental procedures. Mice were stimulated with TLR ligands, and 20 h later, hepatic and splenic leucocytes were analyzed. **(B,C)** Activation of (B) APCs and (C) lymphocytes after treatment with Poly I:C, LPS, ODN 1826, or peptidoglycan ($n = 4$ per group each). MFI, mean fluorescence intensity. Error bars indicate SEM. Differences in MFI were analyzed by the Mann–Whitney test to compare TLR agonists to PBS. Data are representative of two similar independent experiments. **(D)** Cytokine concentrations 20 h after injection of activators of innate immune pathways. PBS (black), ODN 1826 (green), or the ODN 1826 Control (cyan) polynucleotide, LPS (yellow), poly I:C (red), or peptidoglycan (violet). Shown are mean values (+SEM) for each group ($n = 5$ per group, except for ODN 1826 Control, $n = 4$). Data are representative of at least two similar independent experiments. (B-D). *$p < 0.05$; ** $p < 0.01$ (Mann–Whitney).
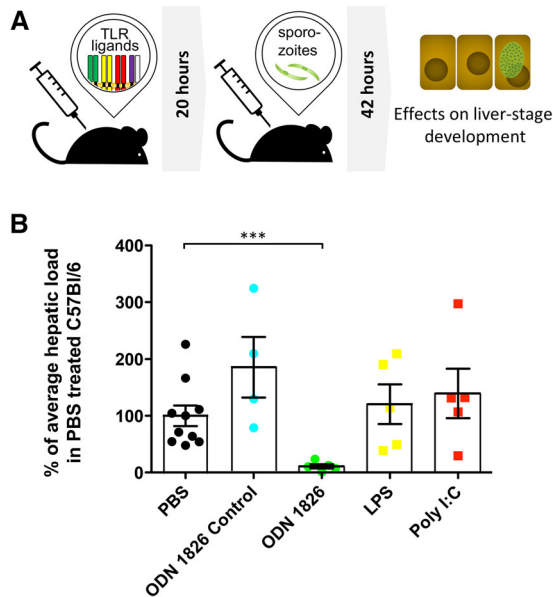
Figure 2. Activation of TLR9 pathway modulates *Pb* liver-stage development. **(A)** Flowchart of experimental procedures. Mice were prestimulated with PBS (black), ODN 1826 (green), or the ODN 1826 Control (cyan) polynucleotide, LPS (yellow), or poly I:C (red), infected with 10^4 *Pb* sporozoites i.v., and analyzed for hepatic parasite load. **(B)** Expression levels of *Pb*18S rRNA as a surrogate of the hepatic parasite load 42 h after infection with 10^4 *Pb* sporozoites. Values are expressed as the percentage of the mean value for the PBS control group (PBS, $n = 10$; ODN 1826 Control, $n = 4$; ODN 1826, LPS and Poly I:C, $n = 5$ per group). Data shown are representative of two independent experiments. Bars indicate mean infection levels ($\pm$SEM). ***$p < 0.001$ (Mann–Whitney).

EEF development in vivo (Fig. 2) or subsequent blood-stage infection (Fig. 6)—inhibited sporozoite motility, which then impacts the development of EEFs in vitro. Using immunofluorescence microscopy to visualize trails of circumsporozoite protein (CSP) shed by the parasite, addition of 100 µM or 20 µM ODN 1826—doses exceeding concentration that the parasite would reasonably encounter in vivo after i.v. administration —reduced the number of trains observed (Fig. 3C); motile parasites were reduced by 83 and 81%, respectively (data not shown). Similarly, the addition of the same concentrations of ODN 1826 Control led to comparable reduction in the trails observed. As we did not observe any differences between ODN 1826 and the ODN 1826 Control, it is unlikely that direct inhibition of parasite motility plays any significant role in reduction of the hepatic parasite load. LPS treatment did not substantially impact sporozoite motility in vitro (Fig. 3C).

Inhibition of *Pb* pre-erythrocytic stages depends on innate activation and IFN-γ

To further analyze the contribution of distinct cytokines to the inhibition of *Pb* pre-erythrocytic stages in the specific setting of the liver, we measured the amounts of transcripts of type I IFN, IFN-γ, IL-12p35, IL-12p40 and IL-10 42 h after infection of pretreated mice (Supporting information Fig. S2). IFN-γ transcripts were upregulated 240-fold in the group that had received ODN 1826,

while all other ligands did not induce such a robust response. Comparable to IFN-γ, we found a 15-fold induction of IL-12 that was restricted to ODN 1826-treated mice. We quantified the abundance of transcripts of IFN-α (by assessing a consensus region of IFN–α 1, -2, -5, -6, -7, -9, -11, -12, and -13) and of IFN-β that synergize with IL-12 to drive cell-mediated immune responses [39]. These IFNs have, for instance, been implicated in the regulation of IFN-γ and iNOS as central players in the early response against the protozoan parasite *Leishmania major* [40]. While we did not observe a differential regulation of IFN-α, we found an upregulation of IFN-β by approximately 35-fold in mice that had received ODN 1826 prior to infection.

These observations of differentially regulated cytokines are consistent with a known role of IL-12 to activate NK cells [41, 42] and T_H1 cells to produce IFN-γ [42] or IFN-γ and IL-10 simultaneously [43]. Using RAG1$^{-/-}$ mice, which are deficient in T (and B) cells, we showed that the innate response elicited by ODN 1826 was not sufficient to significantly reduce the hepatic parasite load ($p = 0.059$; Fig. 4), suggesting a role for T-cell activation in this system. Next, we tested if IFN-γ signalling is required by pretreating mice lacking a functional IFN-γ receptor (IFNGR1$^{-/-}$) with ODN 1826. IFNGR1$^{-/-}$ mice were unable to significantly reduce the parasite load ($p = 0.88$; Fig. 4).

Inhibition of *Pb* pre-erythrocytic stages depends on macrophage activation

Having assessed the importance of IFN-γ induction, we eventually examined the presumed effector cells by broad depletion of mononuclear phagocytes with clodronate liposomes (CL). CL were injected i.p. 2 days prior to ODN 1826 application (Supporting information Fig. 5A). Depletion efficacy was controlled by flow cytometry analysis of peritoneal, splenic and hepatic leucocytes, which revealed the loss of an F4/80$^+$/CD11b$^+$ population after 48 h in animals that received the depletion regimen alongside the experimental animals (Supporting information Fig. S3).

We compared four groups of mice, which received PBS, PBS/ODN 1826, CL, or CL/ODN 1826 (Fig. 5B). Depletion of mononuclear phagocytes ablated the ability of TLR9 activation to induce a reduction of the parasite load in the liver. We observed no significant differences between mice that had received CL plus ODN 1826 and untreated controls or controls that had received CL only ($p > 0.05$). Comparison of untreated mice with mice that had received ODN 1826 but no CL revealed a significant difference ($p = 0.016$), supporting the notion of complete reversion of the antiparasitic effect by CL (Fig. 5B).

The observation that liver-stage inhibition is reversed by broad depletion of phagocytes was consistent with differential alteration of local iNOS transcription (Fig. 5C). In parallel to the determination of hepatic parasite burden, we tested for local iNOS expression levels by quantitative real-time PCR. Prestimulation with ODN 1826 alone led to >10-fold upregulation compared to naïve mice, but we did not observe a significant difference in mice that had received PBS or CL, respectively. Thus, we conclude that *Pb*
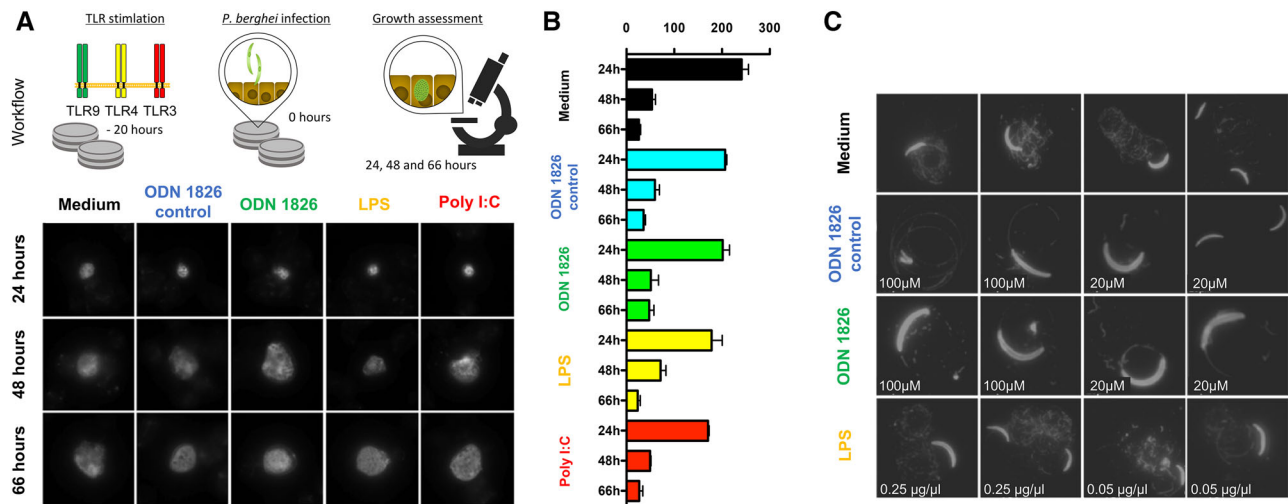
Figure 3. Effect of TLR agonists on *Pb* liver-stage development in vivo and sporozoite gliding motility in vitro. **(A)** Development of exoerythrocytic forms (EEFs). Primary mouse hepatocytes were incubated for 24 h with 2 μM ODN 1826 Control, 2 μM ODN 1826, 10 μg/mL LPS, or 100 μg/mL poly I:C, and infected with 10^4 *Pb* sporozoites. Controls were left untreated. Shown are representative images of EEFs at 24, 48, and 69 h after sporozoite infection. **(B)** Quantification of EEF development in prestimulated primary hepatocytes. Mean values (+SEM) of triplicate samples are indicated. **(A,B)** Data are representative of two similar independent experiments. **(C)** Fluorescent microscopy images of *Pb* sporozoites and gliding trails after incubation with TLR ligands. TLR agonist, and concentration are indicated. Each row shows two representative parasites at two different concentrations. Representative images from two similar independent experiments are displayed.

infection naturally does not upregulate iNOS transcription. Strikingly, CL pretreatment largely reduced the ODN 1826-mediated iNOS overexpression to a threefold increase only (Fig. 5C).

Together, these data establish that the anti-liver stage effects of TLR9 activation can be attributed to increased IFN-γ release by innate and adaptive sources supporting the effector function of hepatic macrophages.
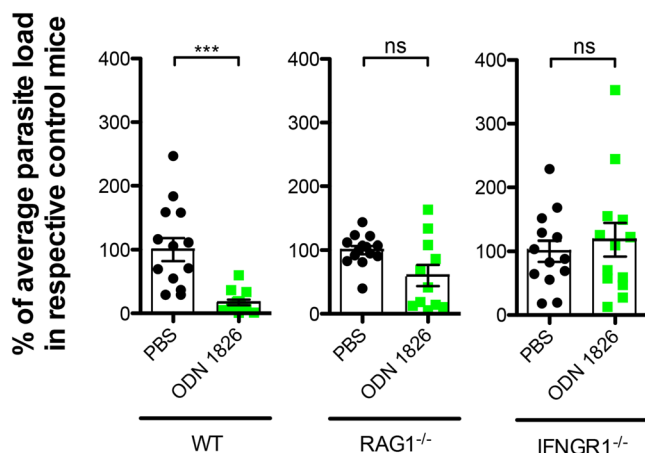

Figure 4. Mechanisms of reduction of hepatic parasite load following TLR9 stimulation. C57Bl/6 WT (*n* = 14), RAG1-/- (*n* = 11), and IFNGR1-/- (*n* = 13) mice were either treated with PBS or ODN 1826 20 h prior to i.p. infection with 10^4 *Pb* sporozoites. The hepatic parasite load was measured with qRT-PCR 42 h later. Data points represent individual animals. Cumulative data from three independent experiments. Bars indicate mean hepatic parasite load (±SEM). ns, not significant. ***$p < 0.001$ (Mann–Whitney).

TLR activation impacts clinical outcome of sporozoite-induced blood-stage infection

To assess whether activation of TLR-pathways prior to inoculation of sporozoites not only affects the pre-erythrocytic stages of the *Pb* life cycle but also the subsequent blood-stage infection, we monitored the time to blood-stage infection, the development of parasitemia, survival, and ECM development in groups of mice treated with ODN 1826, Poly I:C, and LPS compared to ODN 1826 Control or PBS (Fig. 6A). We detected blood-stage parasites in mice in the control groups on 3 to 4 days postinfection (Fig. 6B). In mice treated with ODN 1826, in contrast, blood-stage infections were only detectable significantly later and appeared between days 5 and 7 postinfection (*p* = 0.0034) (Fig. 6B,C). Parasitaemia levels were significantly lower in the ODN 1826-treated animals as compared to the PBS group on days 5 (*p* = 0.0043), 6 (*p* = 0.0022), and 7 (*p* = 0.0043) of the observation period. The apparently low parasitemia observed in the LPS group compared to the PBS group did not reach significance. Application of Poly I:C or peptidoglycan did not significantly affect the time to patency. Despite a longer prepatent period in ODN 1826-treated mice, the rate at which parasitemia increased was similar in all groups once a blood-stage infection had been established (Fig. 6C).

PBS or ODN 1826 Control-treated C57Bl/6 mice developed classical neurological signs of ECM 5–8 days after infection (Fig. 6D). The delayed patency among mice that had received ODN 1826 correlated with a significantly different survival curve from the control groups (*p* = 0.0008, log-rank test) (Fig. 6D), and the majority of the animals were protected against ECM (Fig. 6E). Notably, the survival curve for LPS-treated mice was also significantly different from the control groups (*p* = 0.0008), and the
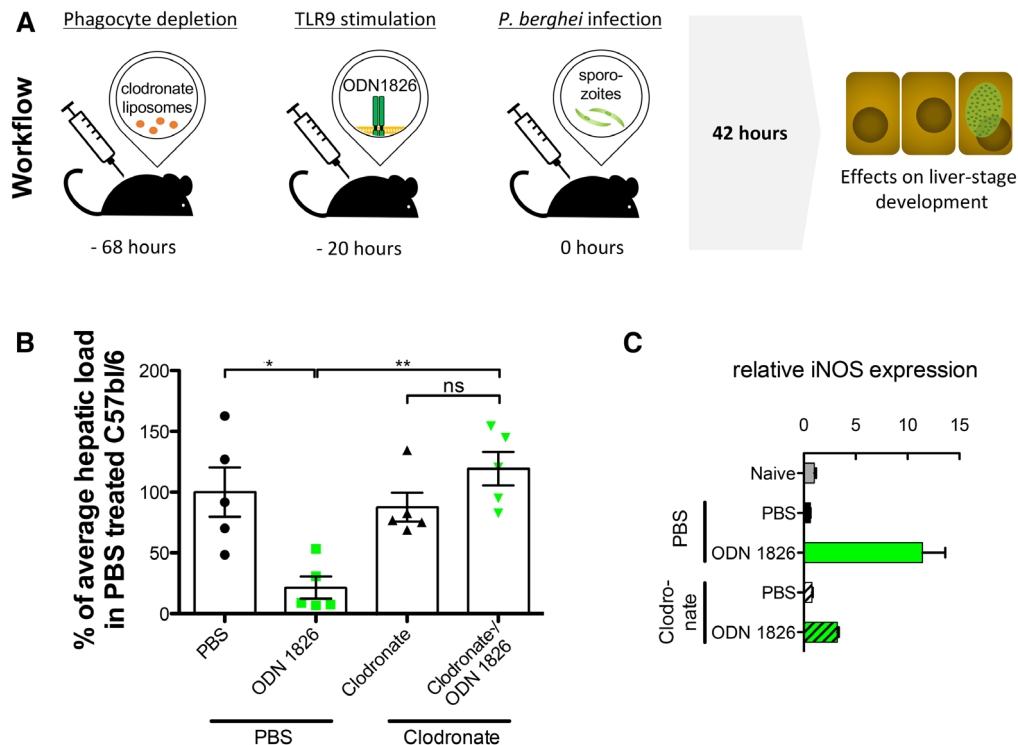
Figure 5. Antiparasitic immune mechanisms induced by TLR9 activation depend on macrophage activity and iNOS expression. **(A)** Flowchart of macrophage depletion experiments. Mice were injected i.p. with 0.1 mL of CL 68 h before infection, prestimulated with PBS or ODN 1826 2 days later and infected with 10^4 *Pb* sporozoites i.v. another 20 h later. After 42 h, the hepatic parasite load was assessed. **(B)** Parasite load in mice treated with CL 2 days prior to injection of ODN 1826 ($n = 5$). Controls were treated with CL and PBS, PBS and CpG, or received injections of PBS only ($n = 5$ per group). Data points represent individual animals; mean values ($\pm$SEM) are displayed. Data are representative of two similar independent experiments. **(C)** Quantitative real-time PCR analysis of hepatic iNOS expression 42 h after infection. Samples from pretreated groups ($n = 5$) or naïve controls ($n = 2$) were pooled and analyzed in technical triplicates. All expression levels are indicated as x-fold of the expression level in naïve mice. Bars indicate mean (+SEM). Data are representative of two independent experiments. *$p < 0.05$; **$p < 0.01$.

majority of the animals were also protected against ECM. Mice that did not succumb to ECM were not protected from developing anemia and high levels of parasitemia.

Cytokine patterns after TLR activation and sporozoite-induced blood-stage infection

We further assessed the serum levels of IFN-γ, TNF, IL-10, IL-6, IL-12p70, and MCP-1 at 0 h (time of infection; as Fig. 1D), 24 h, and 5 days after injection of sporozoites into prestimulated mice. C57Bl/6 mice that developed ECM were shown to exhibit high levels of serum IFN-γ, TNF, and MCP-1 prior to the onset of neurological signs [10, 11, 44]. Consistent with this observation, PBS- and ODN 1826 Control-treated mice had significant increases in these cytokines on day 5 after sporozoite infection (Fig. 7). In contrast, sporozoite-infected mice pretreated with ODN 1826 or LPS had an almost inverted cytokine pattern. Pretreatment with ODN 1826 initiated a robust secretion of IFN-γ at the time of infection and 24 h later. At both time points, average levels observed were more than eightfold higher than in PBS-treated mice. Notably, pretreatment with ODN 1826 prevented the

characteristic peak of IFN-γ levels on day 5 after infection; serum IFN-γ levels were about 15× lower as compared to the control group when it developed ECM. Serum MCP-1 concentrations in ODN 1826-treated mice increased by more than 100× at the time of infection. One day later, MCP-1 concentrations decreased, and it was only slightly elevated on day 5 after infection. No induction of TNF could be detected after administration of ODN 1826. IL-6, IL-10, and IL12p70 levels showed no distinct pattern at the measured time points. Similar to the injection of ODN 1826, pretreatment with LPS led to low serum levels of IFN-γ, MCP-1, and TNF on day 5 after infection, which correlated with the observed protection against ECM. Activation of the TLR3 pathway did not prevent progression to ECM and was associated with an increase in serum IFN-γ, MCP-1, and TNF levels before manifestation of clinical signs.

TLR9 activation impacts clinical outcome following iRBC-initiated infection

We have shown that stimulation with ODN 1826 significantly reduced the hepatic parasite load following sporozoite infection
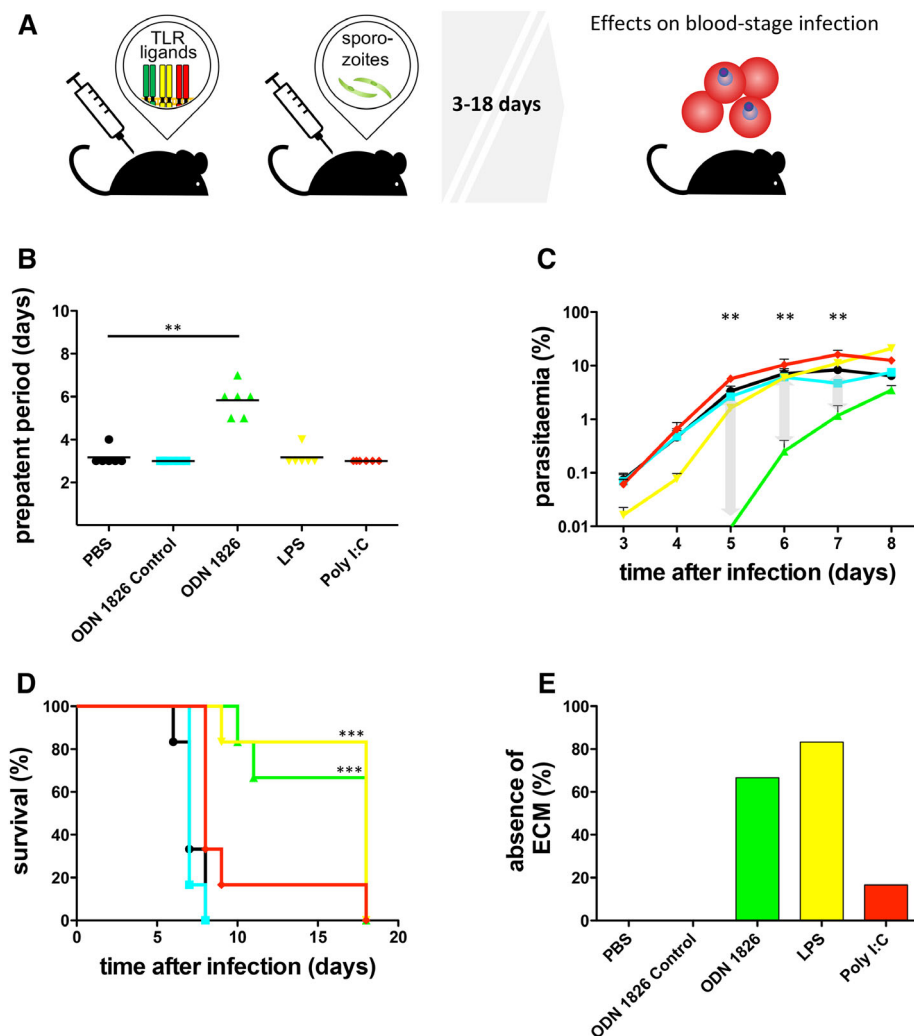
Figure 6. Activation of TLR4 and -9 pathways independently impacts clinical outcome of blood-stage infection following pre-erythrocytic-stage infection. **(A)** Flowchart of experimental procedures. Mice were prestimulated with PBS (black), ODN 1826 (green), or the ODN 1826 Control (cyan) polynucleotide, LPS (yellow) or poly I:C (red), infected with 10^4 *Pb* sporozoites i.v., and analyzed for clinical outcome. **(B)** Time to blood-stage infection after injection of 10^4 *Pb* ANKA sporozoites 20 h after stimulation with the respective reagent. Prepatency was monitored by daily examination of Giemsa-stained blood films ($n =$ 6 per group). **(C)** Mean parasitemia ($\pm$SEM) during the course of infection ($n =$ 6 per group). **(D)** Kaplan–Meier analysis of time from infection to the onset of ECM ($n = 6$ per group). **(E)** Absence of ECM shown as the percentage of infected animals ($n = 6$ per group). (B-E) Data are representative of two similar independent experiments. $^{**}p < 0.01$; $^{***}p < 0.001$.

compared to the control group (Fig. 5B), and this eventually led to delayed prepatency and protection against ECM (Fig. 6). We wanted to explore further whether there is an association between the effects of TLR9 activation on liver-stage development and the reduction in the progression of infected mice to ECM. For this purpose, we evaluated initially the effect of TLR9 activation on iRBC-initiated infection, bypassing the liver stage. We monitored the development of parasitemia, survival and ECM development in groups of mice treated with ODN 1826 or PBS, and infected with iRBCs 20 h later (Fig. 8A). We observed blood-stage parasites in all mice in the control group on day 3 postinfection (Fig. 8B). After treatment with ODN 1826, blood-stage parasites were detectable 4 days after infection in most animals. Parasitaemia levels were significantly lower in the ODN 1826-treated animals as compared to the PBS group on days 4 ($p = 0.0294$), 6 ($p = 0.0284$), and 7 ($p = 0.0286$) of the observation period. Finally, treatment with ODN 1826 conferred significantly longer survival (Fig. 8D; $p = 0.008$) and protection against ECM resulting from iRBC inoculation (Fig. 8E), comparable to sporozoite-induced infections.

Discussion

We systematically assessed the capacity of distinct TLR signalling pathways to influence a subsequent *Plasmodium* infection in the *Pb*ANKA / C57Bl/6 infection model. Infections were initiated with sporozoites to not bypass the obligate liver-stage phases of the life cycle when infections are started with iRBCs. Monitoring the course of infection and profiling the cytokine response during host infection, we found that (i) activation of TLR9 has an inhibitory effect on *Pb* pre-erythrocytic stages, and (ii) the observed inhibition of *Plasmodium* pre-erythrocytic stages was associated with the induction of a proinflammatory environment as exemplified by an early increase of IL-12, IFN-γ, and MCP-1 serum levels and expression. When we assessed underlying mechanisms, we observed that (iii) the inhibitory capacity of TLR9 relies on IFN-γ signalling and that (iv) depletion of $F4/80^+/CD11b^+$ macrophages with CL completely reverses the effect and limits local iNOS overexpression. We also found that (v) while activation of TLR3 did not show any effect against subsequent blood-stage infections, stimulation of TLR4 or -9
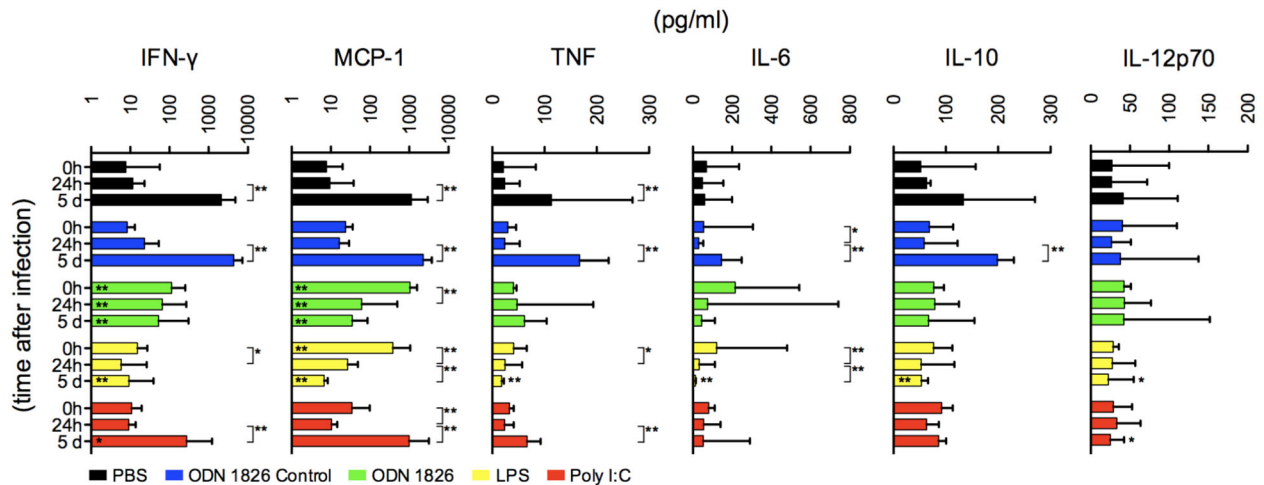
Figure 7. Changes in serum cytokines/chemokine patterns correlate with protection against ECM. Serum samples were collected at the time of infection, 24 h and 5 days postinfection, and the concentrations of IFN-γ, MCP-1, TNF, IL-6, IL-10, and IL-12p70 were measured. Bars indicate median and range for each group at the individual time points. Changes over the course of infection within a group (day 0 versus day 1 and day 1 versus day 5) as well as differences between PBS-treated and agonist-treated mice on day 0, 1, and 5 after infection were assessed. Data are representative of two similar independent experiments. $^*p < 0.05$; $^{**}p < 0.01$ (Mann–Whitney).

in susceptible C57Bl/6 mice prior to challenge with *Pb* ANKA sporozoites significantly reduces the occurrence of ECM; (vi) such protection is associated with suppression of IFN-γ, TNF, and MCP-1 responses at day 5 after infection, before the onset of symptoms. Initial experiments showed that (vii) TLR9 has an inhibitory effect on iRBC-induced infections.

Previous work has established that live homologous or heterologous pathogen infections, that is, by *Plasmodium* sporozoites [45, 46] or enveloped insect baculovirus [47], restrict consecutive *Plasmodium* liver-stage development. This inhibitory effect could be attributed to innate immune activation and type I IFNs, for example, IFN-α, and the type II IFN, IFN-γ, were identified as critical signatures [47]. In the present study, we could show that robust *Plasmodium* liver-stage inhibition can be specifically achieved by prior activation with the TLR9 agonist CpG-DNA, but none of the other agonists. We demonstrate that this trigger of innate defense pathways can occur in the absence of live pathogens and is critically mediated by macrophages, providing a plausible explanation for the previous observation that lys-M-expressing cells are recruited to the liver after induction of IFN signalling [48].

When stimulating C57Bl/6 mice with ODN 1826 prior to challenge with *Pb* ANKA, we observed the capacity of the TLR9 pathway to modulate malaria progression. Inhibition of liver-stage development of *Pb* led to a delay in blood-stage patency, and we report a significantly reduced number of animals that progressed to ECM. While low liver-stage burden is usually associated with a delay in blood-stage patency, it is conceivable that the inflammatory environment—as exemplified by increase in serum levels of IL-12, IFN-γ, and MCP-1—induced following TLR9 activation can also impact blood stages as they egress out of the liver. Nonetheless, our findings that activation of TLR9 has an inhibitory effect on *Pb* pre-erythrocytic stages, are consistent with obser-

vations that an altered, often inflammatory, pre-erythrocytic or early immune response at day 0–1 may change later host immune responses at days 5 and, thereby, reduce the incidence of ECM [49]. When we induced a TLR9-mediated immune response prior to infection with *Pb* iRBCs, which bypasses the liver stages of infection, animals had lower parasitemia and were completely protected against ECM. This suggests common TLR9-induced effector mechanisms affecting both liver and blood stages of infection. Given the limited scope of our experiments with iRBCs, further work is needed to corroborate the direct effects of TLR9 activation on malaria blood stages.

Based on previous reports that CpG ODNs impair sporozoite locomotion by negative charges [38], we tested if direct inhibition of parasites, which bypasses immune signalling via TLR9, plays a principal role in reducing and delaying pre-erythrocytic stages. While we could confirm that CpG ODNs inhibit sporozoite gliding motility, we observed that non-TLR9 binding oligonucleotides have an identical effect on sporozoites in vitro, but have no effect in the course of murine infections. Additionally, we observed in vitro that priming of primary mouse hepatocytes, which have been shown to express TLR1 through -9 [50], with ODN 1826, LPS, poly I:C, or ODN 1826 Control is not sufficient to render them less susceptible to infection with sporozoites. Thus, we conclude that ODN 1826 impairs development of *Pb* pre-erythrocytic stages via the TLR9 immune signalling pathway, involving cells other than hepatocytes. By priming and infecting mice deficient in the common TLR adaptor molecule MyD88, we corroborated that an undisrupted TLR9 signalling pathway is crucial to target *Pb* liver stages with ODN 1826 in vivo.

Intriguingly, we observed that ODN 1826 elicits a cytokine response very similar to a well-known cross-regulatory signalling pathway. Early secretion of IL-12 is known to prompt T cells and NK cells to produce IFN-γ to activate phagocytic effector cells to
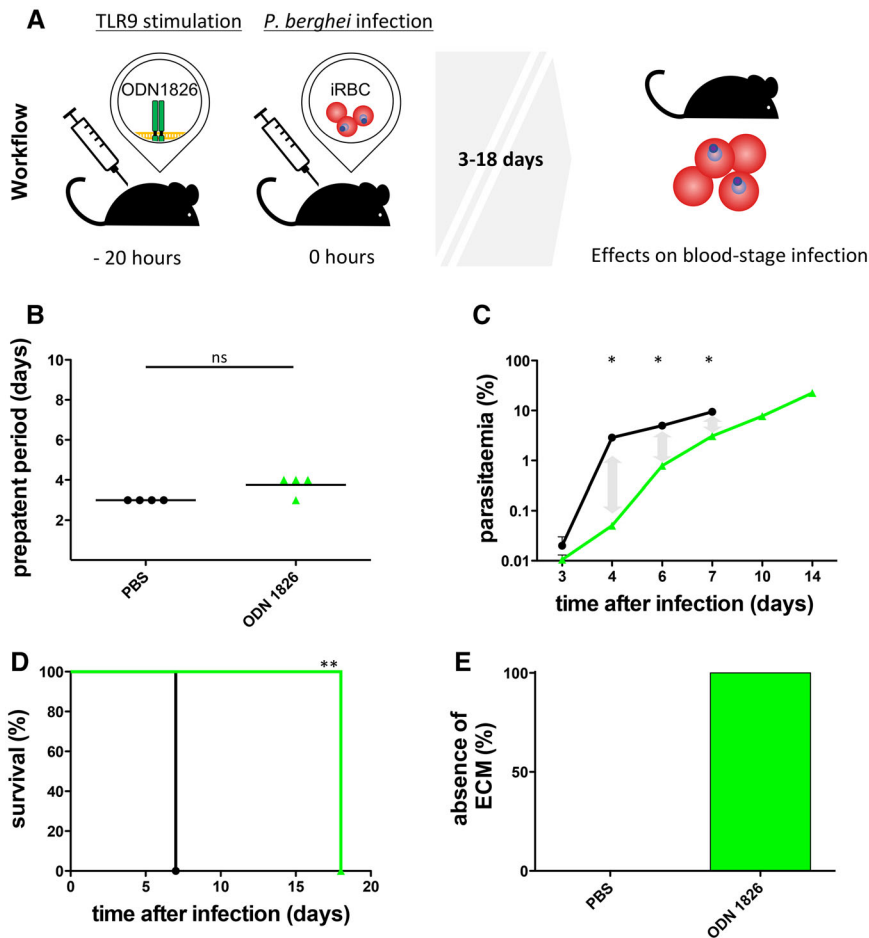
Figure 8. Activation the TLR9 pathway impact clinical outcome of blood-stage infection following infected red blood cell (iRBC) inoculation. **(A)** Flowchart of experimental procedures. Mice were prestimulated with PBS (black) or ODN 1826 (green), inoculated with 10^4 *Pb* iRBC i.v., and analyzed for clinical outcome. **(B)** Time to detection of blood stages after injection of 10^4 *Pb* iRBC 20 h after stimulation with the respective reagent. Prepatency was monitored by daily examination of Giemsa-stained blood films ($n = 4$ per group). **(C)** Mean parasitemia ($\pm$SEM) during the course of infection ($n = 4$ per group). **(D)** Kaplan–Meier analysis of time from infection to the onset of ECM ($n = 4$ per group). **(E)** Absence of ECM shown as the percentage of infected animals ($n = 4$ per group). (B-E) Data are representative of two similar independent experiments. $^*p < 0.05$; $^{**}p < 0.01$.

counter intracellular infection [41]. Activated macrophages, in turn, produce IL-12 to maintain IFN-γ secretion by T cells and NK cells and, thus, feedforward the immune response [41,42]. We assessed this association by testing stimulation with ODN 1826 in RAG1$^{-/-}$ and IFNGR1$^{-/-}$ C57Bl/6 mice. After ODN 1826 stimulation, sporozoite-infected RAG1$^{-/-}$ mice and IFNGR1$^{-/-}$ mice, were unable to significantly reduce the parasite load in the liver. We concluded that (i) IFN-γ is central to the reduction of liver stages via the TLR9 pathway; (ii) sources of IFN-γ could include T and NK cells for the observed reduction; and that (iii) the effect is stronger in the presence of fully competent T cells.

Based on these findings, we hypothesized that activated macrophages are the primary effector cell to mediate *Pb* inhibition. Depletion of mononuclear phagocytes with CL cells led to a complete reversion of the effect of ODN 1826 and a parasite load in the livers, which was comparable to untreated animals. In accordance with this mechanism, which had not yet been implicated in anti-*Plasmodium* liver-stage activity, we observed that transcription of iNOS was locally upregulated in the livers of ODN 1826-treated mice. iNOS catalyses the synthesis of the effector molecule NO from L-arginine in response to pathogens in an IFN-γ-dependent fashion [51,52], and NO is considered a major effector mechanism of host defense against *Plasmodium* in the vector *An. stephensi* [53]. In good accordance, the amount of iNOS tran-

scripts was significantly reduced in the livers of mice depleted of F4/80+/CD11b$^+$ cells. Reduction was, however, not complete, pointing towards iNOS induction in cells, which are not targeted by CL, such as neutrophils [54]. Curiously, and in contrast to earlier studies with the cognate pathogen *P. yoelii* [55], treatment with CL did not lead to enhanced proliferation of liver stages.

We demonstrate for the first time that priming with sublethal doses of LPS significantly reduces ECM-related mortality in susceptible C57Bl/6 mice after infection with *Pb* ANKA. Because we did neither observe any inhibition of liver stage development nor impaired parasite growth during subsequent blood-stage infection, we conclude that LPS modulation of the response to *Pb* infections primarily interferes with *Pb*-induced immunopathology. Based on CD69 expression, LPS potently led to the activation of CD4$^+$ T cells, CD8$^+$ T cells, NK T cells, and NK cells and resulted in a very robust and early peak of serum levels of IL-6. Type I IFN secretion was consistently shown to be an early event in the induction of a potent innate response in the liver and CD49b$^+$CD3$^+$ NK T cells have been implied in the consecutive secretion of IFN-γ [45, 46]. Twenty-four hours after LPS injection, however, regression to very low levels of IFN-γ, TNF and MCP-1 appear to occur, and the dysregulation of these cytokines, characteristic of progression to ECM, was restrained. This observation resembles the hypo-responsiveness

of LPS-primed murine and human macrophages to a second challenge with LPS, a condition termed LPS tolerance, which is known to interfere with TLR4 signalling in multiple ways [56]. Remarkably, a previous investigation found malaria infections in humans and mice to inversely induce hyper-responsiveness to LPS via TLR9-dependent TLR4 over-expression [57]. This ultimately led to increased mortality by sub-lethal doses of LPS in the mouse model. By analogy, we assume that LPS stimulation ablates ECM by a pleiotropic effect, caused by interference with downstream signalling of TLR4. Supporting this hypothesis, TLR4$^{-/-}$ mice have been described to succumb to ECM similar to WT mice [21,58].

Interestingly, the effect of TLR4 and -9 activation on ECM resembles observations in the context of experimental whole-organism vaccine strategies that altered immune responses during the first 2 days after PbANKA infection paradoxically causes reduced inflammation and cerebral pathology 5 to 8 days postinfection [49, 59–62]. In contrast, our observation that TLR9 activation prevents ECM irrespective of the route of infection is counterintuitive to the recent report that depletion of γδ T cells and a liver stage-directed IFN-γ response are associated with protection against ECM following sporozoite but not iRBC infection [63]. However, the exact mechanism by which LPS and CpG DNA prevent progression to ECM and its potential relevance, *for example*, in a bacteria/*Plasmodium* coinfection model remains elusive and the scope of further studies.

Our findings put into perspective the common perception that TLR pathways are primarily involved in malaria-related immunopathology by demonstrating for the first time that activation of TLR4 and -9 pathways can significantly reduce the rate of ECM in mice. As administration of the anti-inflammatory corticoid dexamethasone has been proven to be no more effective than placebo or even deleterious in adjunct therapy of CM [64,65], a more profound understanding of the role of innate immune signalling in severe malaria is warranted to rationally develop adjuvant care to maximize treatment efficacy against the severest form of clinical malaria. Likewise, the identification of innate immune signalling and effector mechanisms that inhibit *Plasmodium* liver-stage development has important implications for interventions that target this bottleneck in the *Plasmodium* life cycle. To date, only experimental whole-organism pre-erythrocytic vaccines confer reliable sterile protection against malaria [6]. Thus, a deeper understanding of innate immune responses against this stage provides means to rationally choose and develop effective adjuvants to improve the antigen-specific immunogenicity of potential subunit vaccines.

Material and methods

Animals

Female C57Bl/6AnNCr mice (6-10 weeks old) were purchased from Charles River Laboratories. Mice deficient in MyD88 (obtained from S. Akira [66]), RAG1 or IFNGR1 in the C57Bl/6

background were bred in a pathogen-free animal facility at the Max-Planck-Institute for Infection Biology and have been back-crossed for at least 10 generations.

Pb ANKA infection

Pb ANKA parasites, which originate from clone 15cy1 that has been engineered to express the green fluorescent protein (GFP) [67], were maintained by regular passage through naïve mice and *Anopheles stephensi* mosquitoes. Groups of C57Bl/6 mice were inoculated by i.v. injection with 10^4 sporozoites, which were freshly purified from mosquito salivary glands. C57Bl/6 mice that had been inoculated with *Pb* parasites were observed daily for the clinical signs of ECM, which was defined by the sudden onset of ataxia, paralysis, convulsion, or coma [9]. Manifestation of ECM signs served as the ethical endpoint criterion for culling affected animals. Infected mice that did not develop ECM until day 18 after infection were considered resistant and culled to avoid suffering from high parasitemia and severe anemia.

Innate immune modulators and pre-treatment

The following agonists were injected i.p. in a total volume of 200 μL saline: ODN 1826 (20 nmol/mouse; Eurofins MWG Operon), LPS from *Escherichia coli* O127:B8 (50 μg/mouse; Sigma), polyinosinic-polycytidylic acid (Poly I:C; 200 μg/mouse; Sigma), or peptidoglycan from *Bacillus subtilis* (50 μg/mouse; Sigma). We included a control oligonucleotide with inverted CpG motifs (ODN 1826 Control) without affinity to TLR9 (20 nmol/mouse; Eurofins MWG Operon) and used 1× PBS (Gibco) as the control for all other agents. All animals were monitored after inoculation for pain, distress, or local complications at the injection site.

Phenotypic analysis of liver and spleen-derived APC and T cells

Mice were sacrificed at indicated time points postinfection, livers were perfused with 1x PBS to remove contaminating intravascular leukocytes, and spleens and livers were removed. Single-cell suspensions from spleens and livers were prepared by homogenizing the organs through a 100-μm cell strainer (BD Biosciences). Leukocytes from liver samples were separated by centrifugation on a 30% isotonic Percoll gradient (GE Healthcare). RBCs were removed from all samples using BD RBC lysis buffer (BD Biosciences), and live cells were quantified using a hemocytometer and trypan blue staining. Phenotypic characterization of cell populations was performed by surface staining according to standard protocols. Antibodies for cell- surface staining were obtained from eBiosciences, BD Biosciences and the German Rheumatism Research Center: anti-mouse CD3 (17A2); anti-mouse CD4 (GK1.5); anti-mouse CD8 (53.6-7), anti-mouse CD11c

(N418); anti-mouse CD49b (DX5); anti-mouse CD69 (H1.2F3); anti-mouse CD80 (16-10A1); anti-mouse CD86 (GL-1); anti-mouse F4/80 (BM8); and anti-mouse MHCII (M5/114.15.2). For flow cytometry quantifications, the following gating strategy on red cells lysed samples was applied: First, the lymphoycte population was identified in a side scatter versus forward scatter density plot; next, the respective percentages of cell populations were determined using different gating methods applied to CD3high cells. Data were acquired by flow cytometry using an LSRFortessa or LSRII (BD) and analyzed using Flowjo9.5.2 (Tree Star, Inc.). For this, we have adhered to the "Guidelines for the use of flow cytometry and cell sorting in immunological studies" [68].

Cell culture

Murine hepatocytes were purified as described elsewhere [69]. Briefly, a single lobe of mouse liver was enzymatically digested and parenchymal cells were suspended in supplemented Williams E medium. After removal of debris on a 60% isotonic Percoll gradient (GE Healthcare), live cells were cultured at 37°C in 4% CO_2 in William's E medium. A total of 10^5 primary hepatocytes were plated in eight-chamber slides (Nunc) and incubated with TLR ligands for at least 24 h before infection with 10^4 *Pb* ANKA sporozoites. Prior to infection, cultures were washed extensively with sterile HBSS (Gibco) to remove immunostimulants in the supernatant. Sporozoites and hepatocytes were incubated for 2 h at room temperature. Cultures were washed again with HBSS and incubated until the indicated time points. After fixation with ice-cold methanol, cultures were stained using a primary mouse monoclonal antibody against *Pb* HSP70 [70]. EEF formation was assessed by comparison of the sizes of the parasites and by quantification of the absolute number of parasites per slide.

Sporozoite gliding assay

Eight-well glass slides were precoated with BSA. A total of 3000 sporozoites in RPMI medium, supplemented with indicated immunostimulants, were deposited in each well and incubated at 37°C for 1 h. The slides were washed and trail deposits were fixed with 4% paraformaldehyde for 15 min. Trails were labeled using polyclonal mouse anti-*Pb*CSP antibodies and a secondary rat anti-mouse antibody conjugated to Alexa Fluor® 647 and visualized by fluorescence microscopy.

Serum cytokine measurement

Serum samples for in vivo measurement of cytokines were prepared from heparinized blood from naïve and infected mice. Cytokines were quantified with the mouse inflammation cytometric bead array kit (BD Bioscience) according to the manufacturer's instructions on a LSR II cell analyzer (BD Bioscience). Raw data were analyzed with FlowJo software (Tree Star).

RNA purification, cDNA preparation, and quantitative real-time PCR

RNA was extracted from homogenized mouse livers using the RNeasy kit (Qiagen) and treated with DNase I (Ambion). cDNA was synthesized using the RETROscript kit (Ambion). We used SYBR green I Master Mix (Applied Biosystems) for quantitative RT-PCR on a StepOne Plus real-time PCR system (Applied Biosystems). Genes of interest were amplified along with the murine housekeeping gene glyceraldehyde 3-phosphate dehydrogenase (*GAPDH*) in a total volume of 25 µL in 96-well plates (Applied Biosystems). Contamination with genomic DNA was excluded by amplification of a nontranscribed target sequence in the CD4 promoter. Oligonucleotide primers (Eurofins MWG Operon) are listed in Supporting information Table S1. Primers for IFNs, IL-10, and IL-12p35/40, as well as the CD4 promoter, have been published previously [71].

Clodronate liposomes

Clodronate liposomes (CL) were prepared as described elsewhere [54]. Briefly, an emulsion of phosphatidylcholin (Sigma) and cholesterol (Sigma) in chloroform was vacuum evaporated. Under inert conditions, a suspension of clodronate (Sigma) was added and encapsulated in multilamellar vesicles by gentle shaking of the reaction vessel. CL were washed with sterile PBS and resuspended in the same buffer solution. We injected 0.1 mL of CL suspension i.p. for depletion experiments.

Statistical analysis

The statistical significance of differences between groups was tested with the Mann–Whitney nonparametric test. Kaplan–Meier curves were compared with the Log-rank test (Mantel–Cox). A *p*-value <0.05 was considered to indicate a significant difference. All statistical analyses were performed with GraphPad Prism 5 (GraphPad Software).

Conflict of interest: The authors declare no conflict of interest.

Author contributions: Conception and design: Maximilian Kordes, Julius Clemence R. Hafalla.

Provision of study materials: Sebastian Rausch.

Collection and assembly of data: Maximilian Kordes, Louise Ormond, Julius Clemence R. Hafalla.

Data analysis and interpretation: Maximilian Kordes, Kai Matuschewski, Julius Clemence R. Hafalla.

Manuscript writing: Maximilian Kordes, Kai Matuschewski, Julius Clemence R. Hafalla.

Final approval of manuscript: All authors.

Accountable for all aspects of the work: All authors.

Peer review: The peer review history for this article is available at https://publons.com/publon/10.1002/eji.202149224

Data availability statement: All data are available from the corresponding author upon reasonable request.

References

1 World Health Organization. World Malaria Report. World Health Organization, Geneva. 2020.

2 Chua, C. L. L., Brown, G., Hamilton, J. A., Rogerson, S. and Boeuf, P., Monocytes and macrophages in malaria: protection or pathology? *Trends Parasitol.* 2013. **29**: 26–34.

3 Langhorne, J., Ndungu, F. M., Sponaas, A.-M. and Marsh, K., Immunity to malaria: more questions than answers. *Nat. Immunol.* 2008. **9**: 725–732.

4 Stevenson, M. M. and Riley, E. M., Innate immunity to malaria. *Nat. Rev. Immunol* 2004. **4**: 169–180.

5 Prudêncio, M., Rodriguez, A. and Mota, M. M., The silent path to thousands of merozoites: the *Plasmodium* liver stage. *Nat. Rev. Microbiol.* 2006. **4**: 849.

6 Hafalla, J. C., Silvie, O. and Matuschewski, K., Cell biology and immunology of malaria. *Immunol. Rev.* 2011. **240**: 297–316.

7 Cowman, A. F., Healer, J., Marapana, D. and Marsh, K., Malaria: biology and disease. *Cell* 2016. **167**: 610–624.

8 van der Heyde, H. C., Nolan, J., Combes, V., Gramaglia, I. and Grau, G. E., A unified hypothesis for the genesis of cerebral malaria: sequestration, inflammation and hemostasis leading to microcirculatory dysfunction. *Trends Parasitol.* 2006. **22**: 503–508.

9 De Souza, J. B., Hafalla, J. C., Riley, E. M. and Couper, K. N., Cerebral malaria: why experimental murine models are required to understand the pathogenesis of disease. *Parasitol* 2010. **137**: 755–772.

10 Amani, V., Vigário, A. M., Belnoue, E., Marussig, M., Fonseca, L., Mazier, D. and Rénia, L., Involvement of IFN-γ receptor-mediated signaling in pathology and anti-malarial immunity induced by *Plasmodium berghei* infection. *Eur. J. Immunol* 2000. **30**: 1646–1655.

11 Grau, G. E., Fajardo, L. F., Piguet, P.-F., Allet, B., Lambert, P.-H. and Vassalli, P., Tumor necrosis factor (cachectin) as an essential mediator in murine cerebral malaria. *Science* 1987. **237**: 1210–1212.

12 Engwerda, C. R., Mynott, T. L., Sawhney, S., De Souza, J. B., Bickle, Q. D. and Kaye, P. M., Locally up-regulated lymphotoxin α, not systemic tumor necrosis factor α, is the principle mediator of murine cerebral malaria. *J. Exp. Med* 2002. **195**: 1371–1377.

13 Hafalla, J., Cockburn, I. and Zavala, F., Protective and pathogenic roles of CD8+ T cells during malaria infection. *Parasite Immunol.* 2006. **28**: 15–24.

14 Rénia, L., Potter, S. M., Mauduit, M., Rosa, D. S., Kayibanda, M., Deschemin, J.-C., Snounou, G. and Grüner, A. C., Pathogenic T cells in cerebral malaria. *Int. J. Parasitol.* 2006. **36**: 547–554.

15 Kawai, T. and Akira, S., Toll-like receptors and their crosstalk with other innate receptors in infection and immunity. *Immunity* 2011. **34**: 637–650.

16 Iwasaki, A. and Medzhitov, R., Toll-like receptor control of the adaptive immune responses. *Nat. Immunol.* 2004. **5**: 987–995.

17 Schwandner, R., Dziarski, R., Wesche, H., Rothe, M. and Kirschning, C. J., Peptidoglycan-and lipoteichoic acid-induced cell activation is mediated by Toll-like receptor 2. *J. Biol. Chem.* 1999. **274**: 17406–17409.

18 Alexopoulou, L., Holt, A. C., Medzhitov, R. and Flavell, R. A., Recognition of double-stranded RNA and activation of NF-κB by Toll-like receptor 3. *Nature* 2001. **413**: 732–728.

19 Poltorak, A., He, X., Smirnova, I., Liu, M.-Y., Van Huffel, C., Du, X., Birdwell D. et al., Defective LPS signaling in C3H/HeJ and C57BL/10ScCr mice: mutations in Tlr4 gene. *Science* 1998. **282**: 2085–2088.

20 Hemmi, H., Takeuchi, O., Kawai, T., Kaisho, T., Sato, S., Sanjo, H., Matsumoto, M. et al., A Toll-like receptor recognizes bacterial DNA. *Nature* 2000. **408**: 740–745.

21 Togbe, D., Schofield, L., Grau, G. E., Schnyder, B., Boissay, V., Charron, S., Rose S. et al., Murine cerebral malaria development is independent of Toll-like receptor signaling. *Am. J. Pathol.* 2007. **170**: 1640–1648.

22 Lepenies, B., Cramer, J. P., Burchard, G. D., Wagner, H., Kirschning, C. J. and Jacobs, T., Induction of experimental cerebral malaria is independent of TLR2/4/9. *Med Microbiol. Immunol.* 2008. **197**: 39–44.

23 Baccarella, A., Huang, B. W., Fontana, M. F. and Kim, C. C., Loss of Toll-like receptor 7 alters cytokine production and protects against experimental cerebral malaria. *Malaria J.* 2014. **13**.

24 Coban, C., Ishii, K. J., Uematsu, S., Arisue, N., Sato, S., Yamamoto, M., Kawai T. et al., Pathological role of Toll-like receptor signaling in cerebral malaria. *Int. Immunol.* 2006. **19**: 67–79.

25 Kordes, M., Matuschewski, K. and Hafalla, J. C., Caspase-1 activation of interleukin-1beta (IL-1beta) and IL-18 is dispensable for induction of experimental cerebral malaria. *Infect. Immun.* 2011. **79**: 3633–3641.

26 Coban, C., Ishii, K. J., Kawai, T., Hemmi, H., Sato, S., Uematsu, S., Woods A. S. et al., Toll-like receptor 9 mediates innate immune activation by the malaria pigment hemozoin. *J. Exp. Med.* 2005. **201**: 19–25.

27 Krishnegowda, G., Hajjar, A. M., Zhu, J., Douglass, E. J., Uematsu, S., Akira, S. et al., Induction of proinflammatory responses in macrophages by the glycosylphosphatidylinositols of *Plasmodium falciparum*: cell signaling receptors, glycosylphosphatidylinositol (GPI) structural requirement, and regulation of GPI activity. *J. Biol. Chem.* 2005. **280**: 8606–8616.

28 Parroche, P., Lauw, F. N., Goutagny, N., Latz, E., Monks, B. G., Visintin, A., Halmen K. A. et al., Malaria hemozoin is immunologically inert but radically enhances innate responses by presenting malaria DNA to Toll-like receptor 9. *Proc. Natl Acad. Sci. USA* 2007. **104**: 1919–1924.

29 Franklin, B. S., Ishizaka, S. T., Lamphier, M., Gusovsky, F., Hansen, H., Rose, J., Zheng W. et al., Therapeutical targeting of nucleic acid-sensing Toll-like receptors prevents experimental cerebral malaria. *Proc. Natl Acad. Sci. USA* 2011. **108**: 3689–3694.

30 Tse, K. and Horner, A. A., Update on Toll-like receptor-directed therapies for human disease. *Ann. Rheum. Dis.* 2007. **66**: iii77–iii80.

31 Chen, J., Xu, W., Zhou, T., Ding, Y., Duan, J. and Huang, F., Inhibitory role of Toll-like receptors agonists in *Plasmodium yoelii* liver stage development. *Parasite Immunol.* 2009. **31**: 466–473.

32 Gramzinski, R. A., Doolan, D. L., Sedegah, M., Davis, H. L., Krieg, A. M. and Hoffman, S. L., Interleukin-12-and gamma interferon-dependent protection against malaria conferred by CpG oligodeoxynucleotide in mice. *Infect. Immun.* 2001. **69**: 1643–1649.

33 Frevert, U. and Krzych, U., *Plasmodium* cellular effector mechanisms and the hepatic microenvironment. *Front Microbiol* 2015. **6**: 482–482.

34 Steers, N., Schwenk, R., Bacon, D. J., Berenzon, D., Williams, J. and Krzych, U., The immune status of Kupffer cells profoundly influences their responses to infectious *Plasmodium berghei* sporozoites. *Eur. J. Immunol.* 2005. **35**: 2335–2346.

35 Tavares, J., Formaglio, P., Thiberge, S., Mordelet, E., Van Rooijen, N., Medvinsky, A., Ménard R. et al., Role of host cell traversal by the malaria sporozoite during liver infection. *J. Exp. Med.* 2013. **210**: 905–915.

36 Schnare, M., Holt, A. C., Takeda, K., Akira, S. and Medzhitov, R., Recognition of CpG DNA is mediated by signaling pathways dependent on the adaptor protein MyD88. *Curr. Biol.* 2000. **10**: 1139–1142.

37 Hacker, H., Vabulas, R. M., Takeuchi, O., Hoshino, K., Akira, S. and Wagner, H., Immune cell activation by bacterial CpG-DNA through myeloid differentiation marker 88 and tumor necrosis factor receptor-associated factor (TRAF)6. *J. Exp. Med.* 2000. **192**: 595–600.

38 Liehl, P., França, A. R., Prudêncio, M., Latz, E., Zaidman-Rémy, A. and Mota, M. M., Phosphothioate oligodeoxynucleotides inhibit *Plasmodium* sporozoite gliding motility. *Cell. Microbiol.* 2010. **12**: 506–515.

39 González-Navajas, J. M., Lee, J., David, M. and Raz, E., Immunomodulatory functions of type I interferons. *Nat. Rev. Immunol.* 2012. **12**: 125–135.

40 Diefenbach, A., Schindler, H., Donhauser, N., Lorenz, E., Laskay, T., MacMicking, J., Röllinghoff M. et al., Type 1 interferon (IFNα/β) and type 2 nitric oxide synthase regulate the innate immune response to a protozoan parasite. *Immunity* 1998. **8**: 77–87.

41 Chace, J. H., Hooker, N. A., Mildenstein, K. L., Krieg, A. M. and Cowdery, J. S., Bacterial DNA-induced NK cell IFN-γ production is dependent on macrophage secretion of IL-12. *Clin. Immunol. Immunopathol.* 1997. **84**: 185–193.

42 Seder, R. A., Gazzinelli, R., Sher, A. and Paul, W. E., Interleukin 12 acts directly on CD4+ T cells to enhance priming for interferon gamma production and diminishes interleukin 4 inhibition of such priming. *Proc. Natl Acad. Sci. USA* 1993. **90**: 10188–10192.

43 Windhagen, A., Anderson, D., Carrizosa, A., Williams, R. and Hafler, D., IL-12 induces human T cells secreting IL-10 with IFN-gamma. *J. Immunol.* 1996. **157**: 1127–1131.

44 Hanum, P., Hayano, M. and Kojima, S., Cytokine and chemokine responses in a cerebral malaria-susceptible or-resistant strain of mice to *Plasmodium berghei* ANKA infection: early chemokine expression in the brain. *Int. Immunol.* 2003. **15**: 633–640.

45 Miller, J. L., Sack, B. K., Baldwin, M., Vaughan, A. M. and Kappe, S. H. I., Interferon-mediated innate immune responses against malaria parasite liver stages. *Cell Rep.* 2014. **7**: 436–447.

46 Liehl, P., Meireles, P., Albuquerque, I. S., Pinkevych, M., Baptista, F., Mota, M. M., Davenport, M. P. and Prudêncio, M., Innate immunity induced by *Plasmodium* liver infection inhibits malaria reinfections. *Inf Immun* 2015. **83**: 1172–1180.

47 Emran, T. B., Iyori, M., Ono, Y., Amelia, F., Yusuf, Y., Islam, A., Alam A. et al., *Baculovirus*-induced fast-acting innate immunity kills liver-stage *Plasmodium*. *J. Immunol.* 2018. **201**: 2441–2451.

48 Liehl, P., Zuzarte-Luis, V., Chan, J., Zillinger, T., Baptista, F., Carapau, D., Konert M. et al., Host-cell sensors for *Plasmodium* activate innate immunity against liver-stage infection. *Nat. Med.* 2014. **20**: 47–53.

49 Fernandes, P., Frank, R., Lewis, M. D. and Mueller, A.-K., *Plasmodium* attenuation: connecting the dots between early immune responses and malaria disease severity. *Front. Microbiol.* 2014. **5**: 658.

50 Liu, S., Gallo, D. J., Green, A. M., Williams, D. L., Gong, X., Shapiro, R. A., Gambotto A. A. et al., Role of toll-like receptors in changes in gene expression and NF-κB activation in mouse hepatocytes stimulated with lipopolysaccharide. *Infect. Immun.* 2002. **70**: 3433–3442.

51 Fang, F. C. Mechanisms of nitric oxide-related antimicrobial activity. *J. Clin. Invest.* 1997. **99**: 2818–2825.

52 Rosenberger, C. M., Scott, M. G., Gold, M. R., Hancock, R. E. and Finlay, B. B., *Salmonella typhimurium* infection and lipopolysaccharide stimulation induce similar changes in macrophage gene expression. *J. Immunol.* 2000. **164**: 5894–5904.

53 Whitten, M., Shiao, S.-H. and Levashina, E., Mosquito midguts and malaria: cell biology, compartmentalization and immunology. *Parasite Immunol.* 2006. **28**: 121–130.

54 Van Rooijen, N. and Sanders, A., Liposome mediated depletion of macrophages: mechanism of action, preparation of liposomes and applications. *J. Immunol. Methods* 1994. **174**: 83–93.

55 Baer, K., Roosevelt, M., Clarkson Jr, A. B., Van Rooijen, N., Schnieder, T. and Frevert, U., Kupffer cells are obligatory for *Plasmodium yoelii* sporozoite infection of the liver. *Cell. Microbiol.* 2007. **9**: 397–412.

56 Dobrovolskaia, M. A. and Vogel, S. N., Toll receptors, CD14, and macrophage activation and deactivation by LPS. *Microbes Infect.* 2002. **4**: 903–914.

57 Franklin, B. S., Parroche, P., Ataíde, M. A., Lauw, F., Ropert, C., de Oliveira, R. B., Pereira D. et al., Malaria primes the innate immune response due to interferon-γ induced enhancement of toll-like receptor expression and function. *Proc. Natl Acad. Sci. USA* 2009. **106**: 5789–5794.

58 Griffith, J. W., O'connor, C., Bernard, K., Town, T., Goldstein, D. R. and Bucala, R., Toll-like receptor modulation of murine cerebral malaria is dependent on the genetic background of the host. *J. Infect. Dis.* 2007. **196**: 1553–1564.

59 Friesen, J., Silvie, O., Putrianti, E. D., Hafalla, J. C., Matuschewski, K. and Borrmann, S., Natural immunization against malaria: causal prophylaxis with antibiotics. *Sci. Transl. Med.* 2010. **2**: 40ra49–40ra49.

60 Gerald, N. J., Majam, V., Mahajan, B., Kozakai, Y. and Kumar, S., Protection from experimental cerebral malaria with a single dose of radiation-attenuated, blood-stage *Plasmodium berghei* parasites. *PLoS One* 2011. **6**: e24398.

61 Haussig, J. M., Matuschewski, K. and Kooij, T. W., Inactivation of a *Plasmodium* apicoplast protein attenuates formation of liver merozoites. *Mol. Microbiol.* 2011. **81**: 1511–1525.

62 Lewis, M. D., Behrends, J., Sá e Cunha, C., Mendes, A. M., Lasitschka, F., Sattler, J. M., Heiss K. et al., Chemical attenuation of *Plasmodium* in the liver modulates severe malaria disease progression. *J. Immunol.* 2015. **194**: 4860–4870.

63 Ribot, J. C., Neres, R., Zuzarte-Luís, V., Gomes, A. Q., Mancio-Silva, L., Mensurado, S., Pinto-Neves D. et al., γδ-T cells promote IFN-γ–dependent *Plasmodium* pathogenesis upon liver-stage infection. *Proc. Natl Acad. Sci. USA* 2019. **116**: 9979–9988.

64 Hoffman, S. L., Rustama, D., Punjabi, N. H., Surampaet, B., Sanjaya, B., Dimpudus, A. J., McKee K. T. Jr, et al., High-dose dexamethasone in quinine-treated patients with cerebral malaria: a double-blind, placebo-controlled trial. *J. Infect. Dis.* 1988. **158**: 325–331.

65 Warrell, D. A., Looareesuwan, S., Warrell, M. J., Kasemsarn, P., Intaraprasert, R., Bunnag, D. and Harinasuta, T., Dexamethasone proves deleterious in cerebral malaria: a double-blind trial in 100 comatose patients. *N. Engl. J. Med.* 1982. **306**: 313–319.

66 Adachi, O., Kawai, T., Takeda, K., Matsumoto, M., Tsutsui, H., Sakagami, M., Nakanishi, K. and Akira, S., Targeted disruption of the MyD88 gene results in loss of IL-1-and IL-18-mediated function. *Immunity* 1998. **9**: 143–150.

67 Franke-Fayard, B., Trueman, H., Ramesar, J., Mendoza, J., van der Keur, M., van der Linden, R. et al., A *Plasmodium berghei* reference line that constitutively expresses GFP at a high level throughout the complete life cycle. *Mol. Biochem. Parasitol.* 2004. **137**: 23–33.

68 Cossarizza, A., Chang, H. D., Radbruch, A., Acs, A., Adam, A., Adam-Klages, S., Agace, W. et al., Guidelines for the use of flow cytometry and cell sorting in immunological studies (second edition). *Eur. J. Immunol.* 2019. **49**: 1457–1973.

69 Renia, L., Mattei, D., Goma, J., Pied, S., Dubois, P., Miltgen, F. et al., A malaria heat-shock-like determinant expressed on the infected hepatocyte surface is the target of antibody-dependent cell-mediated cytotoxic mechanisms by nonparenchymal liver cells. *Eur. J. Immunol.* 1990. **20**: 1445–1449.

70 Tsuji, M., Mattei, D., Nussenzweig, R. S., Eichinger, D. and Zavala, F., Demonstration of heat-shock protein 70 in the sporozoite stage of malaria parasites. *Parasitol. Res.* 1994. **80**: 16–21.

71 Gautier, G., Humbert, M., Deauvieau, F., Scuiller, M., Hiscott, J., Bates, E. E., Trinchieri, G. et al., A type I interferon autocrine-paracrine loop is involved in Toll-like receptor-induced interleukin-12p70 secretion by dendritic cells. *J. Exp. Med.* 2005. **201**: 1435–1446.

Abbreviations: **CD**: cluster of differentiation · **CL**: clodronate liposomes · **CM**: cerebral malaria · **ECM**: experimental cerebral malaria · **IFN-γ**: interferon gamma · **iRBC**: infected red blood cell · **LT**: lymphotoxin · **MyD88**: myeloid differentiation primary response protein 88 · **ODN**: oligodeoxynucleotide · *Pb*: *Plasmodium berghei* · **rRNA**: ribosomal ribonucleic acid

Full correspondence: Dr. Julius C. R. Hafalla, Department of Infection Biology, Faculty of Infectious and Tropical Diseases, London School of Hygiene and Tropical Medicine, London, United Kingdom.
e-mail: Julius.Hafalla@lshtm.ac.uk

Current address: Maximilian Kordes, Department of Clinical Science, Intervention and Technology, Karolinska Institutet, 141 86 Stockholm, Sweden.

Current address: Louise Ormond, University College London Genetics Institute, London WC1E 6BT, United Kingdom.